

Electronic Supplementary Information

Photophysical, electrochemical properties and flexible organic solar cell application of 7,7-bis(1-cyclopropyl carbonyl piperazino)-8,8 dicyanoquinodimethane

Anwarhussaini Syed,^a Renuka H,^b Anuradha Mohitkar,^a Raghavaiah Pallepogu,^c Mahadev Karthik Challa,^a Sanket Goel,^b Subbalakshmi Jayanty^{a*}

Fig. S1a ¹ H NMR of BCCPDQ.	S2
Fig. S1b ¹³ C NMR of BCCPDQ.	S2
Fig. S1 c Mass spectrum of BCCPDQ	S3
Fig. S2 ORTEP molecular diagram	S3
Table S1 Basic crystallographic data of BCCPDQ.	S4
Table S2-S6. Detailed crystallographic tables	S5-S9
Fig. S3 (a) Extensive H-bonding network and (b) Supramolecular assemblies	S9
Table S7. Significant non-covalent intermolecular interactions (Å)	S10
Table S8. Absorption, emission stoke shift table and quantum yields	S10
Table S9. Shows the viscosity data of the solvents considered in this study.	S11
Fig. S4 Variable temperature (from 0 to 30 °C) emission spectra in isopropanol (IPA)	S11
Fig. S5 Viscosity study in glycerol-water mixture	S12
Fig S6. Decrease in the emission intensity on adding water to the DMF solution of BCCPDQ indicate aggregation quenching phenomenon.	S12
Fig. S7 Fluorescence lifetime decay	S13
Table S10. Lifetime decay pattern of BCCPDQ	S13
Fig. S8 Scanning electron microscopy images of the drop casted films	S14
Table S11. A comparative table representing the efficiencies in small molecules based solar cells	S14-S15

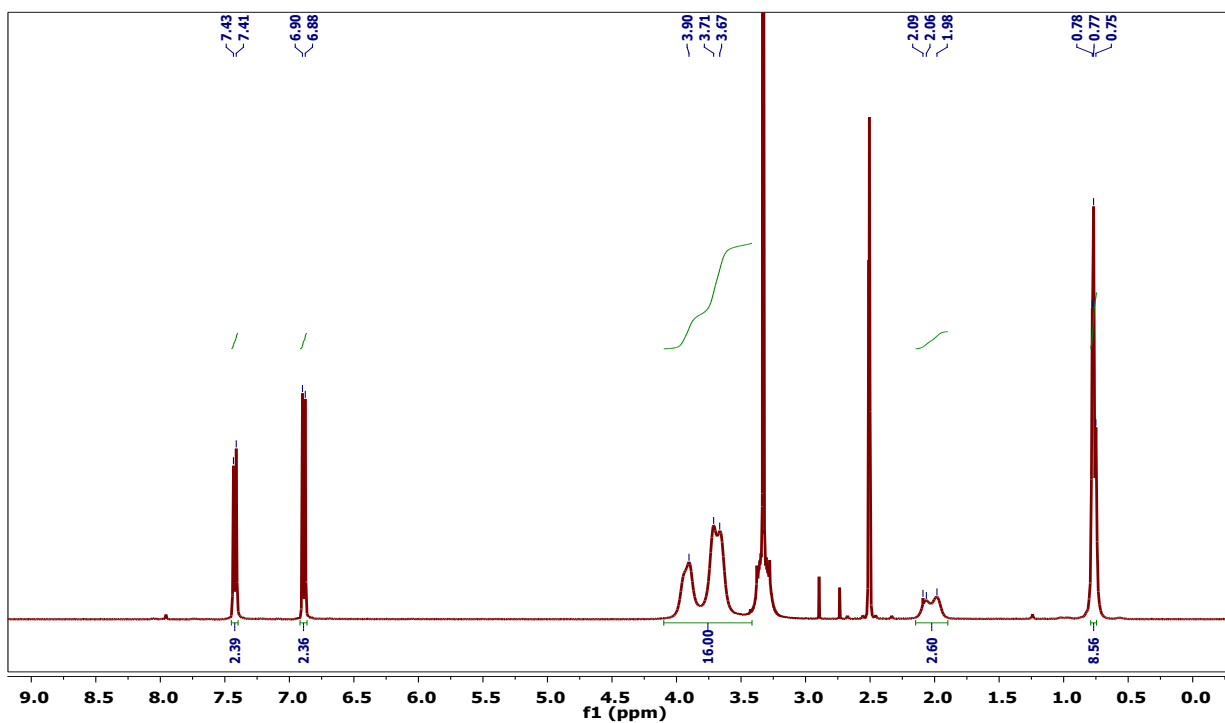


Fig. S1a ¹H NMR of BCCPDQ.

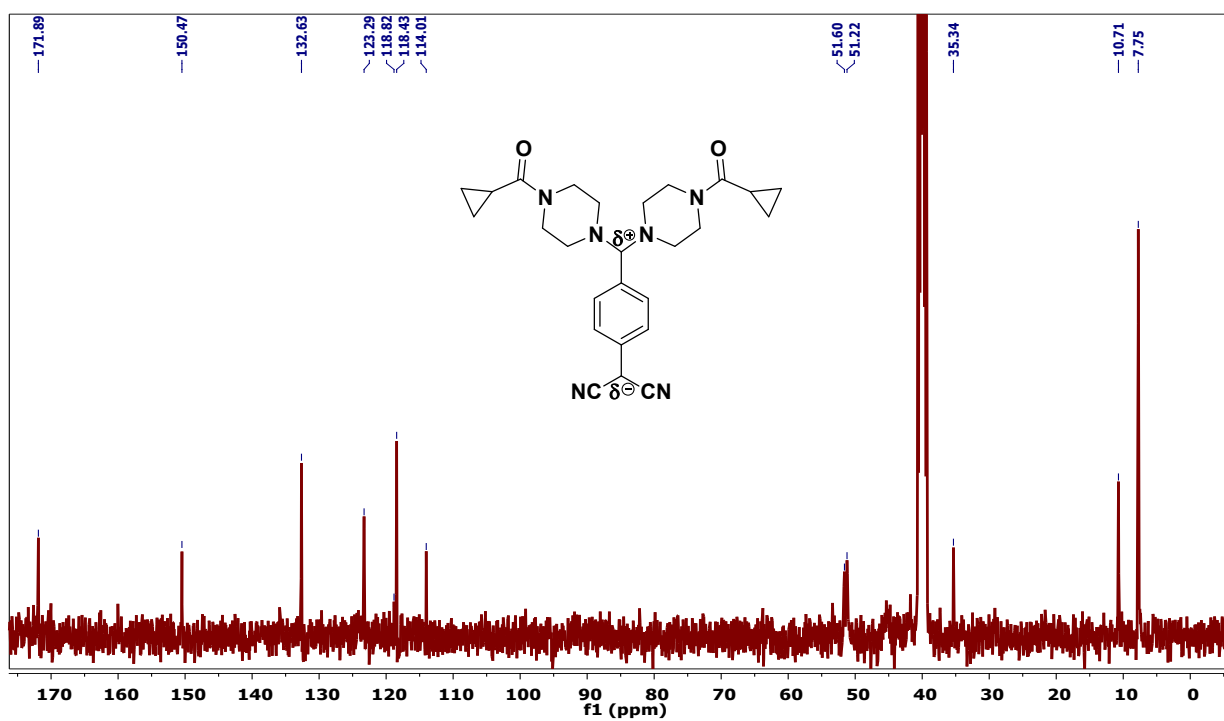


Fig. S1b ¹³C NMR of BCCPDQ.

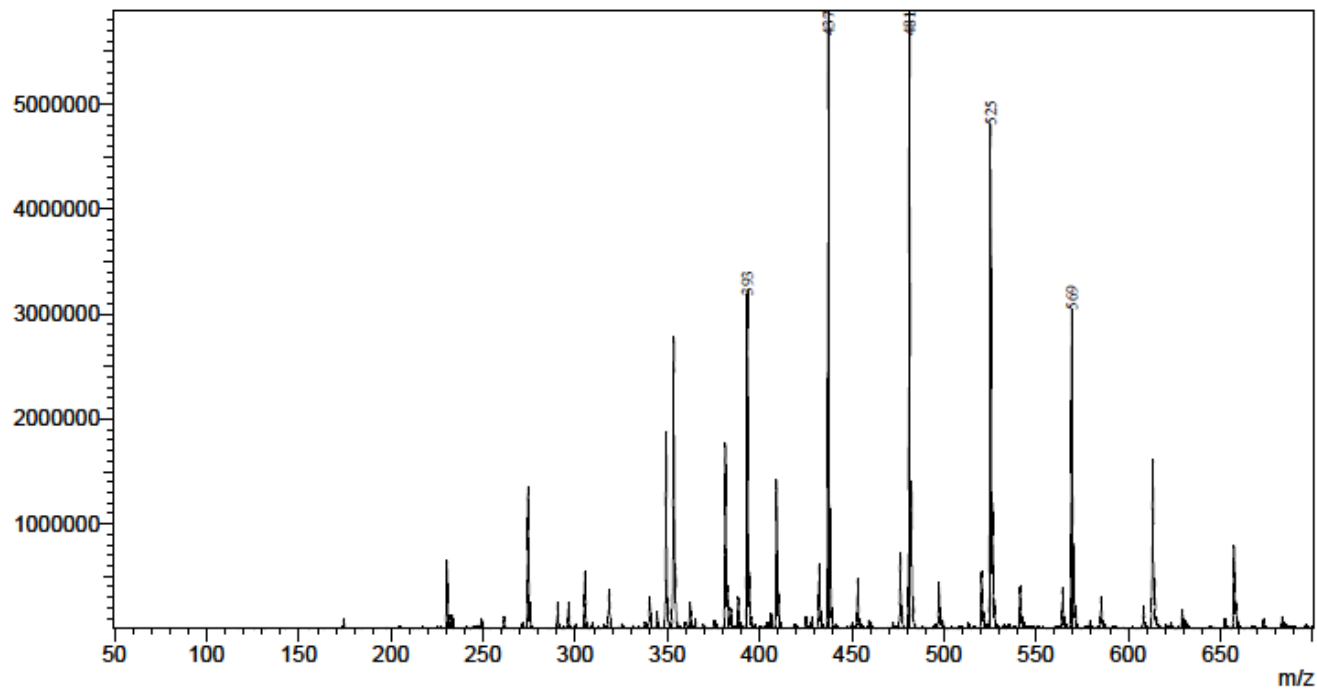


Fig. S1c Mass spectrum of BCCPDQ.

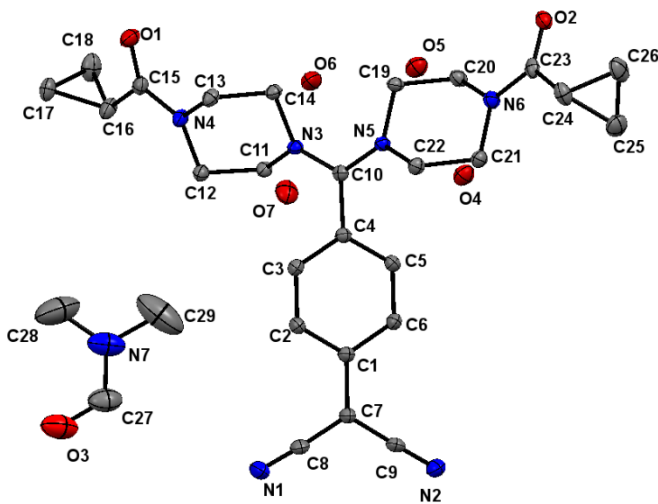


Fig. S2 ORTEP molecular diagram with 50% probability thermal ellipsoids. H-atoms omitted for clarity.

Table S1 Basic crystallographic data of BCCPDQ.

Compound	BCCPDQ
----------	--------

Table
Atomic
(×104)

S2.

Empirical formula	C ₂₉ H ₄₅ N ₇ O ₇			Fractional Coordinates and
Formula weight	603.72			
Temperature/K	293(2)			
Crystal system	x	triclinic	z	
Space group	13369.3(14)	4194.9(8)	4541.5(7)	24.6(2)
a/Å, b/Å, c/Å	5032.5(13)	1117.804(7)	13.6400(3)	15.8558(4)
α/°, β/°, γ/°	10694(2)	5793.700(19)	841267.2(8)	76.169(2)
Volume/Å ³	10184.9(19)	9116.0(7)	-2025.7(8)	25.8(3)
Z	10725.3(14)	6903.8(8)	2862.1(7)	14.2(2)
ρ _{calc} /cm ³	12709.4(15)	4981.20(9)	3325.3(7)	18.1(2)
μ/mm ⁻¹	8278.1(14)	8200.8(8)	2909.7(7)	14.5(2)
R(σ)	6104.5(15)	10164.7(9)	3545.3(7)	18.7(2)
Crystal size/mm	1088.3(18)	7537.5(10)	109.32 × 0.28	9.4(8)
Radiation	10185.0(19)	6645.6(10)	λ = 0.71073	(9)
2θ range for data collection/°	6669.9(18)	7508.2(10)	52.744	1080.8(8)
Index ranges	9726.5(17)	7588.4(10)	-9, -15 ≤ h ≤ 9, -19 ≤ l ≤ 19	13.0(3)
Reflections collected	8613.6(18)	8480.0(10)	1080.4(8)	16.4(3)
Independent reflections	9793.4(19)	8457.6(10)	R _{int} = 0.0515, R _{sigma} = 0.0095	18.1(3)
Data/restraints/parameters	10283.7(19)	7503.8(10)	-1180.6(9)	18.8(3)
Goodness-of-fit on F ²	10323(2)	6577.3(11)	-1619.7(9)	20.7(3)
Final R indexes [I > 2σ(I)]	10228.4(19)	8383.1(11)	R ₁ = 0.0455, wR ₂ = 0.1229	19.1(3)
Final R indexes [all data]	9563.5(17)	7595.3(10)	R ₁ = 0.0480, wR ₂ = 0.1250	14.1(3)
Largest diff. peak/hole / e Å ⁻³	12579.8(17)	6511.6(10)	0.88 / -0.39	15.7(3)
CCDC	2017949			
C12	13100.2(18)	5355.6(10)	2481.1(9)	18.3(3)
C13	10850.6(18)	5357.8(10)	3657.4(9)	18.1(3)
C14	10332.3(17)	6510.4(10)	3710.3(8)	16.0(3)
C15	13874.1(19)	4397.0(10)	3810.8(9)	18.6(3)
C16	15738.3(19)	3985.6(11)	3441.0(10)	23.9(3)
C17	16694(2)	2962.7(11)	3746.4(10)	24.0(3)
C18	17182(2)	3887.3(12)	4027.1(12)	30.4(4)
C19	8355.3(17)	8615.6(10)	3786.1(8)	16.3(3)
C20	7842.1(18)	9767.4(10)	3847.4(9)	18.9(3)
C21	6023.4(18)	9839.4(10)	2674.2(9)	18.3(3)
C22	6536.2(17)	8688.5(10)	2598.3(9)	16.8(3)
C23	4803.4(18)	10824.6(10)	4026.4(9)	17.9(3)
C24	3057.6(19)	11166.0(11)	3664.7(10)	23.2(3)
C25	2738(2)	12112.6(13)	3160.6(11)	30.8(4)
C26	1787(2)	12116.4(13)	4017.4(11)	32.0(4)
O3	5725(2)	1392.4(15)	-1012.9(10)	59.2(4)
N7	4918(2)	2302.7(17)	206.9(11)	51.6(5)
C27	5123(3)	2230(2)	-631.3(13)	48.3(5)
C28	5339(4)	1456(3)	733.4(18)	86.1(10)
C29	4259(4)	3290(3)	631(2)	96.4(12)
O4	2201.3(15)	9048.2(9)	2545.6(7)	26.6(2)
O5	2711.9(15)	8343.2(9)	4180.0(7)	27.6(2)
O6	5671.0(19)	6672.8(10)	3972.5(7)	36.4(3)
O7	6815.2(16)	6197.6(9)	2298.5(8)	32.9(3)

Equivalent Isotropic Displacement Parameters ($\text{\AA}^2 \times 10^3$) for exp_309. U_{eq} is defined as 1/3 of the trace of the orthogonalised UIJ tensor.

Table S3. Anisotropic Displacement Parameters ($\text{\AA}^2 \times 10^3$) for exp_309. The Anisotropic displacement factor exponent takes the form: $-2\pi^2[h^2a^2U_{11}+2hka^*b^*U_{12}+\dots]$.

Atom	U11	U22	U33	U23	U13	U12
O1	24.5(5)	27.0(5)	20.3(5)	6.1(4)	-3.5(4)	-2.1(4)
O2	22.3(5)	17.7(5)	21.1(5)	-2.4(4)	2.3(4)	-2.9(4)
N1	47.9(9)	22.5(7)	19.4(6)	-3.3(5)	0.6(6)	-7.4(6)

N2	37.3(7)	22.0(6)	18.7(6)	3.2(5)	-3.6(5)	-8.1(5)
N3	13.8(5)	15.6(5)	12.4(5)	1.1(4)	-0.2(4)	-2.3(4)
N4	17.2(6)	16.9(5)	18.8(6)	4.3(4)	-0.8(4)	-1.8(4)
N5	13.6(5)	16.6(5)	12.5(5)	-0.3(4)	-2.3(4)	-1.8(4)
N6	16.6(6)	18.4(6)	18.9(6)	-1.5(4)	-2.0(4)	0.3(4)
C1	19.1(6)	17.7(6)	12.8(6)	0.0(5)	-2.0(5)	-4.5(5)
C2	23.1(7)	14.6(6)	15.7(6)	-1.7(5)	-1.4(5)	-3.7(5)
C3	19.4(6)	14.7(6)	15.6(6)	1.9(5)	-1.6(5)	-3.7(5)
C4	15.0(6)	16.7(6)	13.2(6)	0.4(5)	-1.9(5)	-3.2(5)
C5	19.4(6)	14.6(6)	15.2(6)	-1.4(5)	-2.2(5)	-3.9(5)
C6	24.5(7)	14.5(6)	15.8(6)	2.2(5)	-3.1(5)	-5.1(5)
C7	26.2(7)	16.4(6)	13.3(6)	0.1(5)	-1.7(5)	-4.5(5)
C8	27.5(7)	21.7(7)	12.3(6)	1.7(5)	-0.7(5)	-5.3(6)
C9	23.6(7)	21.5(7)	12.0(6)	-2.5(5)	-1.9(5)	-5.1(5)
C10	14.2(6)	14.8(6)	14.3(6)	0.4(5)	-1.5(5)	-5.4(5)
C11	13.5(6)	17.0(6)	15.4(6)	1.9(5)	0.3(5)	-1.9(5)
C12	18.9(6)	17.5(6)	16.4(6)	1.8(5)	-0.5(5)	-0.6(5)
C13	16.3(6)	19.1(7)	18.7(6)	4.6(5)	-1.2(5)	-4.2(5)
C14	15.5(6)	19.0(6)	12.7(6)	2.3(5)	-0.5(5)	-2.6(5)
C15	20.7(7)	13.9(6)	21.7(7)	1.8(5)	-4.3(5)	-3.9(5)
C16	20.4(7)	21.3(7)	27.9(8)	9.0(6)	-2.0(6)	-1.1(6)
C17	20.4(7)	17.7(7)	32.2(8)	4.2(6)	-4.4(6)	-0.3(5)
C18	20.6(7)	24.5(8)	47.5(10)	2.7(7)	-9.7(7)	-5.8(6)
C19	15.8(6)	19.7(7)	11.9(6)	-1.1(5)	-1.1(5)	-1.3(5)
C20	16.6(6)	20.3(7)	18.1(6)	-3.5(5)	-2.1(5)	-1.0(5)
C21	17.1(6)	18.4(7)	18.0(7)	1.0(5)	-3.8(5)	-0.9(5)
C22	13.2(6)	19.1(6)	17.4(6)	0.3(5)	-3.5(5)	-1.8(5)
C23	17.6(6)	11.7(6)	24.1(7)	2.0(5)	1.7(5)	-4.7(5)
C24	17.4(7)	19.3(7)	32.3(8)	-6.2(6)	-2.4(6)	-2.9(5)
C25	32.9(8)	28.3(8)	31.1(8)	2.8(6)	-13.9(7)	-3.0(7)
C26	23.3(8)	28.5(8)	38.3(9)	-8.5(7)	-7.9(7)	7.3(6)
O3	45.7(9)	90.6(13)	35.8(8)	-8.4(8)	-7.1(6)	-4.5(8)
N7	37.3(9)	86.6(14)	32.5(9)	-7.8(9)	-1.4(7)	-18.9(9)
C27	37.0(10)	73.3(15)	33.1(10)	0.8(10)	1.5(8)	-12.3(10)
C28	72.5(19)	135(3)	47.0(15)	27.2(17)	-12.9(13)	-14.9(19)
C29	68.0(19)	121(3)	100(2)	-64(2)	23.3(17)	-35.0(19)
O4	25.7(6)	28.5(6)	26.0(6)	4.0(5)	-8.0(4)	-5.1(5)
O5	27.1(6)	30.6(6)	26.1(6)	3.1(5)	-7.6(4)	-6.9(5)
O6	47.1(8)	32.4(6)	21.5(6)	1.3(5)	-7.9(5)	8.3(6)
O7	27.9(6)	32.0(6)	34.5(6)	0.9(5)	8.7(5)	-3.5(5)

Table S4. Bond Lengths for BCCPDQ.

Atom	Atom	Length/Å	Atom	Atom	Length/Å
O1	C15	1.2381(18)	C4	C5	1.4025(18)

O2	C23	1.2354(18)	C4	C10	1.4746(17)
N1	C8	1.157(2)	C5	C6	1.3814(19)
N2	C9	1.159(2)	C7	C8	1.406(2)
N3	C10	1.3412(17)	C7	C9	1.4045(19)
N3	C11	1.4730(16)	C11	C12	1.5285(18)
N3	C14	1.4777(16)	C13	C14	1.5247(18)
N4	C12	1.4614(17)	C15	C16	1.488(2)
N4	C13	1.4619(17)	C16	C17	1.5182(19)
N4	C15	1.3578(18)	C16	C18	1.513(2)
N5	C10	1.3327(17)	C17	C18	1.481(2)
N5	C19	1.4753(16)	C19	C20	1.5241(19)
N5	C22	1.4743(16)	C21	C22	1.5239(18)
N6	C20	1.4626(17)	C23	C24	1.501(2)
N6	C21	1.4632(17)	C24	C25	1.499(2)
N6	C23	1.3534(18)	C24	C26	1.500(2)
C1	C2	1.4091(19)	C25	C26	1.481(3)
C1	C6	1.4128(19)	O3	C27	1.256(3)
C1	C7	1.4530(18)	N7	C27	1.324(3)
C2	C3	1.3828(19)	N7	C28	1.416(4)
C3	C4	1.4017(19)	N7	C29	1.458(4)

Table S5. Bond Angles for BCCPDQ.

Atom	Atom	Atom	Angle/°	Atom	Atom	Atom	Angle/°
C10	N3	C11	122.41(11)	N5	C10	C4	120.14(11)
C10	N3	C14	124.29(11)	N3	C11	C12	111.52(11)
C11	N3	C14	113.18(10)	N4	C12	C11	109.58(11)
C12	N4	C13	112.44(11)	N4	C13	C14	111.32(11)
C15	N4	C12	127.28(12)	N3	C14	C13	108.66(11)
C15	N4	C13	120.18(11)	O1	C15	N4	120.02(13)
C10	N5	C19	124.27(11)	O1	C15	C16	121.06(13)
C10	N5	C22	122.53(11)	N4	C15	C16	118.91(12)
C22	N5	C19	112.84(10)	C15	C16	C17	116.97(12)
C20	N6	C21	112.89(11)	C15	C16	C18	117.53(14)
C23	N6	C20	121.03(12)	C18	C16	C17	58.50(10)
C23	N6	C21	125.89(12)	C18	C17	C16	60.56(10)
C2	C1	C6	117.55(12)	C17	C18	C16	60.93(10)
C2	C1	C7	120.80(12)	N5	C19	C20	109.68(11)
C6	C1	C7	121.65(12)	N6	C20	C19	110.75(11)
C3	C2	C1	121.20(12)	N6	C21	C22	110.08(11)
C2	C3	C4	120.78(12)	N5	C22	C21	110.81(11)
C3	C4	C5	118.53(12)	O2	C23	N6	122.03(13)
C3	C4	C10	119.98(12)	O2	C23	C24	121.28(12)
C5	C4	C10	121.49(12)	N6	C23	C24	116.68(12)
C6	C5	C4	120.80(12)	C25	C24	C23	118.45(13)
C5	C6	C1	121.14(12)	C25	C24	C26	59.20(11)
C8	C7	C1	119.98(12)	C26	C24	C23	118.68(13)

C9	C7	C1	121.47(12)	C26	C25	C24	60.44(10)
C9	C7	C8	118.55(12)	C25	C26	C24	60.36(11)
N1	C8	C7	176.51(15)	C27	N7	C28	123.1(2)
N2	C9	C7	178.65(15)	C27	N7	C29	120.1(3)
N3	C10	C4	118.74(11)	C28	N7	C29	116.8(3)
N5	C10	N3	121.12(12)	O3	C27	N7	121.4(2)

Table S6. Hydrogen Atom Coordinates ($\text{\AA}\times 104$) and Isotropic Displacement Parameters ($\text{\AA}^2\times 103$) for BCCPDQ.

Atom	x	y	z	U(eq)
H2	10372	6029	-85	22
H3	10074	6071	1373	20
H5	9420	9095	1372	20
H6	9718	9059	-85	22
H11A	13357	6764	2843	19
H11B	12734	6756	1933	19
H12A	12444	5099	2080	22
H12B	14356	5119	2298	22
H13A	10658	5092	4217	22
H13B	10101	5121	3292	22
H14A	9078	6745	3897	19
H14B	10997	6753	4116	19
H16	16036	4143	2849	29
H17A	16042	2627	4160	29
H17B	17527	2513	3340	29
H18A	18314	3999	3792	36
H18B	16830	4114	4612	36
H19A	9546	8366	3948	20
H19B	7549	8344	4172	20
H20A	7811	9986	4432	23
H20B	8727	10035	3510	23
H21A	6827	10117	2291	22
H21B	4831	10091	2516	22
H22A	5644	8417	2925	20
H22B	6581	8481	2010	20
H24	2526	10630	3480	28
H25A	3675	12472	3091	37
H25B	2060	12134	2678	37
H26A	529	12140	4057	38
H26B	2144	12478	4470	38
H27	4814	2813	-945	58
H28A	5927	868	392	129
H28B	4268	1346	1029	129

H28C	6106	1581	1137	129
H29A	5161	3436	946	145
H29B	3224	3283	1011	145
H29C	3959	3799	216	145
H4A	2903	8875	2097	40
H4B	1420(30)	9593(19)	2424(15)	51(7)
H5A	3272	8664	4468	41
H5B	2647	8644	3710	41
H6A	5888	6357	4427	55
H6B	4710(40)	7160(20)	4082(17)	59(7)
H7A	7554	5628	2215	49
H7B	6524	6303	2827	49

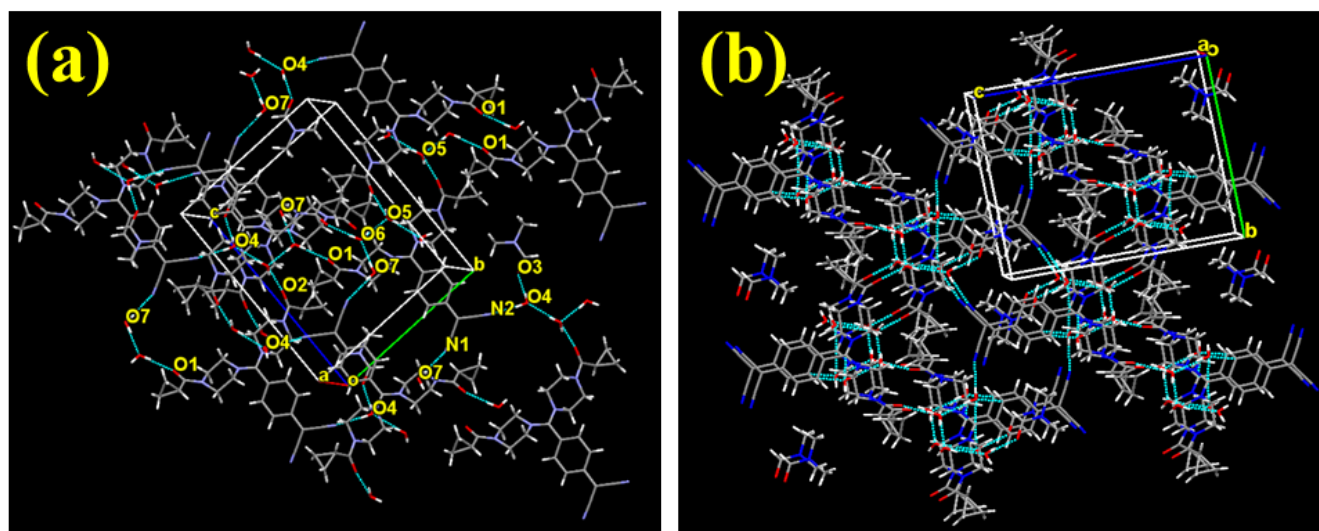


Fig. S3 (a) Extensive H-bonding network among the molecular dipoles of BCCPDQ manifested through the surrounding water and DMF molecules (b) Supramolecular assemblies of molecular dipoles with extensive short contacts.

Table S7. Significant non-covalent intermolecular interactions (Å) and hydrogen bond type ranging from weak, moderate to strong leading to the orientations of molecular dipoles consequently resulting in solid-state fluorescence.

Interaction	C---O-H	N---H-C	N---O-H	O---O-H	H---O-C	C---H-C	O---H-C	H---H-C/H---H-O	N---H-O	O---H-O
H-bond		2.647 2.722 2.746 2.743	2.908 2.953	2.795 2.726 2.765 2.794 2.821 2.742			2.477, 2.664 2.500, 2.529 2.676, 2.719 2.665, 2.669		2.031 2.157	1.886 1.962 1.960 1.888
Short contacts	3.185 3.220 3.188 3.213				2.547	2.892 2.869 2.723		2.388 2.128 2.369		

Table S8. Absorption, emission wavelengths, stoke shift table and quantum yields of BCCPDQ in both solution and solid states.

S.No	Solvent	Absorption maximum (nm)	Emission maximum (nm)	Stoke shift (nm)	QY (%)
1	MeCN	430	535	105	0.13
2	MeOH	423	528	105	0.16
3	EtOH	432	531	99	0.2
4	IPA	442	525	83	0.28
5	DMF	431	526	95	0.21
6	DMSO	425	526	101	0.34
7	SOLID	464	528	64	9.82

Table S9. Shows the viscosity data of the solvents considered in this study.

S.No.	Solvent	Viscosity in centipoise (cp)	Viscosity in centistokes (cst)	Relative polarity
1	Acetonitrile	0.37	0.47	0.46
2	Methanol	0.54	0.69	0.762
3	Ethanol	1.07	1.36	0.654
4	<i>i</i> -propyl alcohol (IPA)	2.04	2.61	0.546
5	DMF	0.79	0.84	0.386
6	DMSO	1.99	1.82	0.444

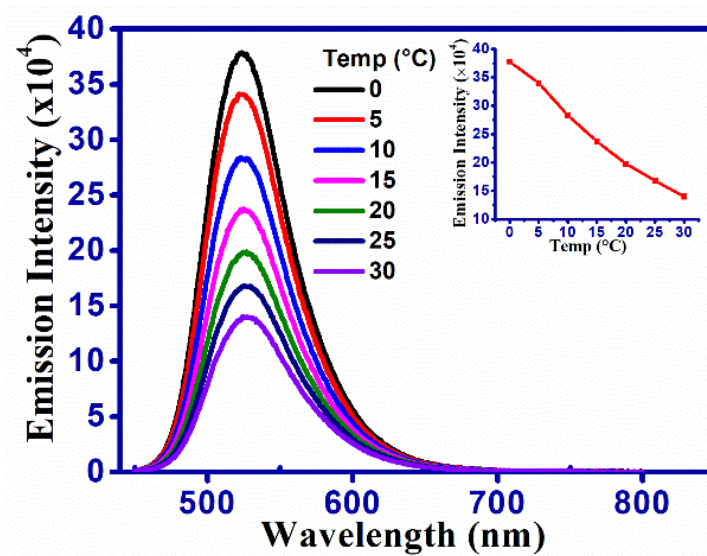


Fig. S4 Variable temperature emission spectra of BCCPDQ in isopropanol (IPA) from 0 to 30 °C.

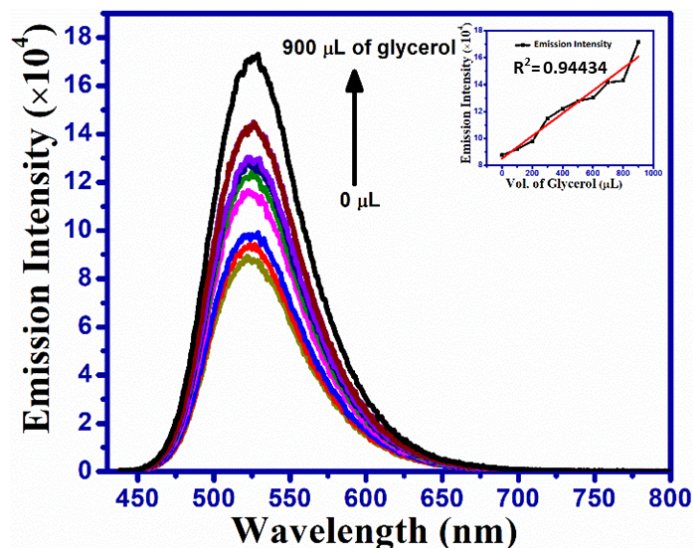


Fig. S5 Viscosity study carried out in the 10 ppm of sample solution, considered in glycerol:water (1:1 volume ratio) mixture. Enhanced emission intensity observed on the gradual increment of 100 μL of glycerol to the initial solutions.

0.5 mg of the BCCPDQ dissolved in a 1:1 volume ratio of glycerol and water mixture, sonicated for about 5 to 10 mins. This solution comprised of 100 ppm concentration, further diluted to 10 ppm and to this 10 ppm solution, at each instant 100 μL of glycerol was added. Fluorescence enhancement noticed with increased amounts of glycerol added (Fig. S6).

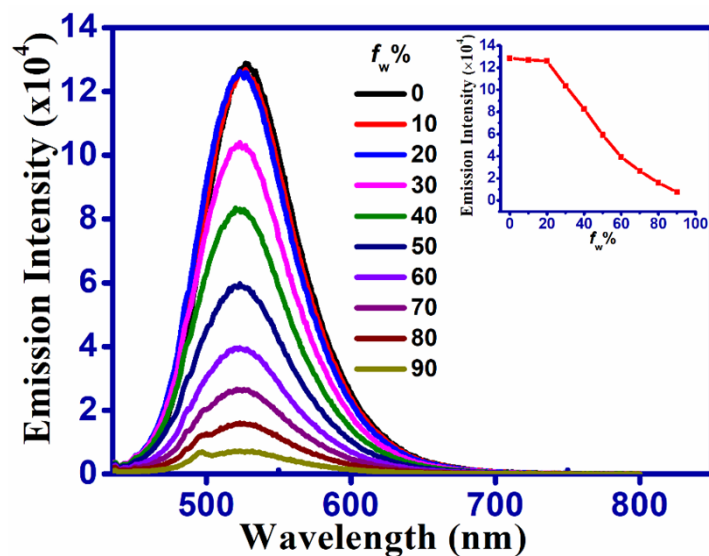


Fig. S6 Decrease in the emission intensity on adding water from 0 to 90% to the 10 ppm DMF solution of BCCPDQ indicating aggregation quenching phenomenon.

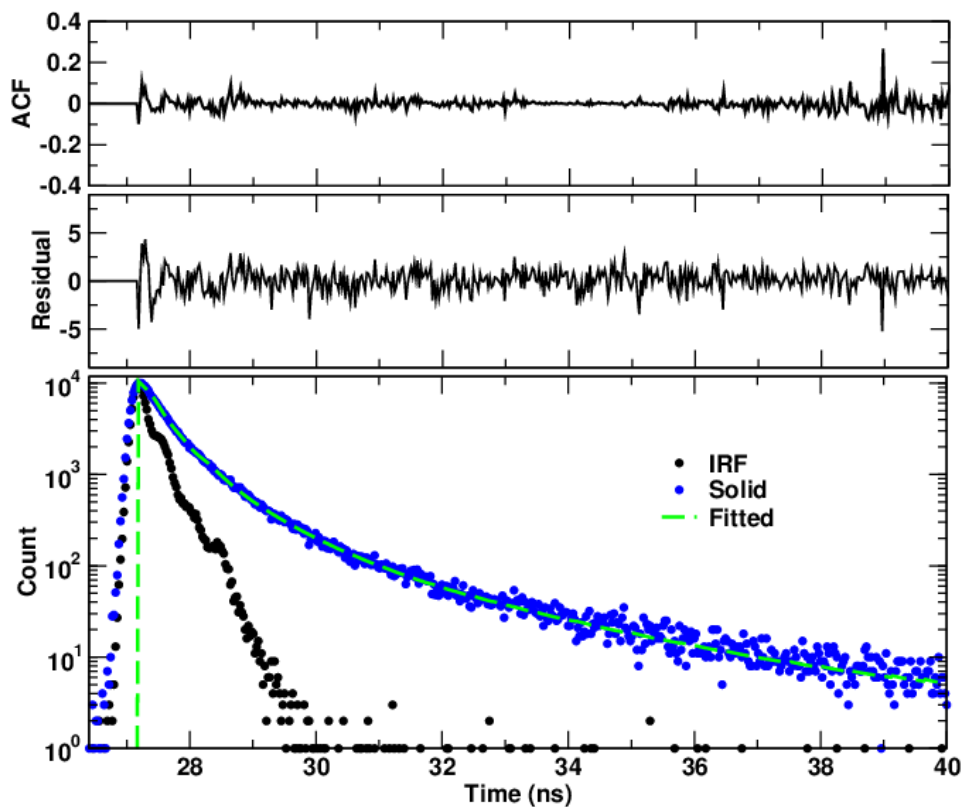


Fig. S7 Shows fluorescence lifetime decay (~ 0.26 ns) for solid ($\lambda_{\max \text{ exc}}$: 464 nm and $\lambda_{\max \text{ emi}}$: 528 nm) along with the residual plot and autocorrelation function (ACF).

Table S10. Lifetime decay pattern of solid BCCPDQ, B_1 , B_2 and B_3 are relative contributions to τ_1 , τ_2 and τ_3 . $\langle \tau \rangle$ is average lifetime from multiple decay profiles.

BCCPDQ (Solid)	$\lambda_{\max \text{ exc}}$ (nm)	$\lambda_{\max \text{ em}}$ (nm)	B_1	B_2	B_3	τ_1	τ_2	τ_3	$\langle \tau \rangle$ (ns)	χ^2	K_r (ns^{-1})	K_{nr} (ns^{-1})
	464	528	0.08	0.01	0.92	0.82	2.67	0.18	0.26	1.34	0.377	0.034

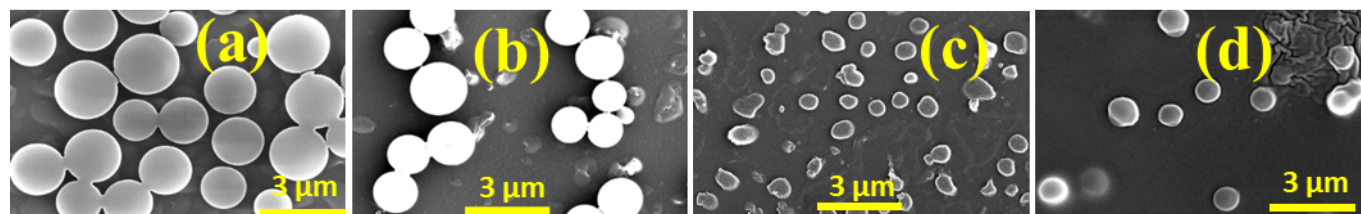


Fig. S8 Scanning electron microscopy images of the drop casted films at 3 μm magnification obtained from the solutions of (a) MeCN, (b) MeOH, (c) EtOH and (d) IPA.

Table S11. A comparative table representing the efficiencies of other recently developed small organic materials based solar cell applications.

Device	Jsc (mA/cm ²)	Voc (V)	PCE (%)	Reference
ITO/pentacene/CuPc/C60/BCP/Al	3.58	0.39	0.79	[1]
ITO/MoO ₃ /CuPc/C60/BCP/Al	3.41	0.39	0.72	[1]
J52:IEICO with 12% TCNQ	0.51	0.650	0.01	TCNQ is applied as a volatilizable additive into the J52:IEICO-based active layer [2]
Al/chlorophyll-a/Hg	--	--	0.001	[3]
Pentacene/C60	8.8		1.6	[4]
SubPc/C60	3.36	0.97	2.1	[5]
DRTB-FT:F-2Cl	10.77	1.098	5.65	This is the as casted device [6]
ITO/PEDOT:PSS/SMPV1:PC71BM/Ca/Al	11.4	0.93	7.2	[7]
Al/BCCPDQ/ITO-PET	2.56	0.5	0.40	Current work
Al/BCCPDQ/TiO₂ NP_s/ITO-PET	6.72	1	2.26	Current work

References

- [1] Huang, P.H., Huang, C.J., Chen, K.L., Ke, J.C., Wang, Y.H. and Kang, C.C., 2014. Improved reliability of small molecule organic solar cells by double anode buffer layers. *Journal of Nanomaterials*, 2014.
- [2] Yu, R., Yao, H., Hong, L., Gao, M., Ye, L. and Hou, J., 2020. TCNQ as a volatilizable morphology modulator enables enhanced performance in non-fullerene organic solar cells. *Journal of Materials Chemistry C*, 8(1), pp.44-49.
- [3] Tang, C.W. and Albrecht, A.C., 1975. Photovoltaic effects of metal–chlorophyll-a–metal sandwich cells. *The Journal of chemical physics*, 62(6), pp.2139-2149.
- [4] Pandey, A.K. and Nunzi, J.M., 2006. Efficient flexible and thermally stable pentacene/C 60 small molecule based organic solar cells. *Applied Physics Letters*, 89(21), p.213506.

- [5] Mutolo, K., E. Mayo, B. Rand, S. Forrest, and M. Thompson. 2006. Enhanced open-circuit voltage in subphthalocyanine=C60 organic photovoltaic cells. *Journal of the American Chemistry Association* 128(25):8108–8109
- [6] Liu, C., Qiu, N., Sun, Y., Ke, X., Zhang, H., Li, C., Wan, X. and Chen, Y., 2020. All-small-molecule organic solar cells based on a fluorinated small molecule donor with high open-circuit voltage of 1.07 V. *Frontiers in chemistry*, 8, p.329.
- [7] Liu, Y., Chen, C.C., Hong, Z., Gao, J., Yang, Y.M., Zhou, H., Dou, L., Li, G. and Yang, Y., 2013. Solution-processed small-molecule solar cells: breaking the 10% power conversion efficiency. *Scientific reports*, 3(1), pp.1-8.